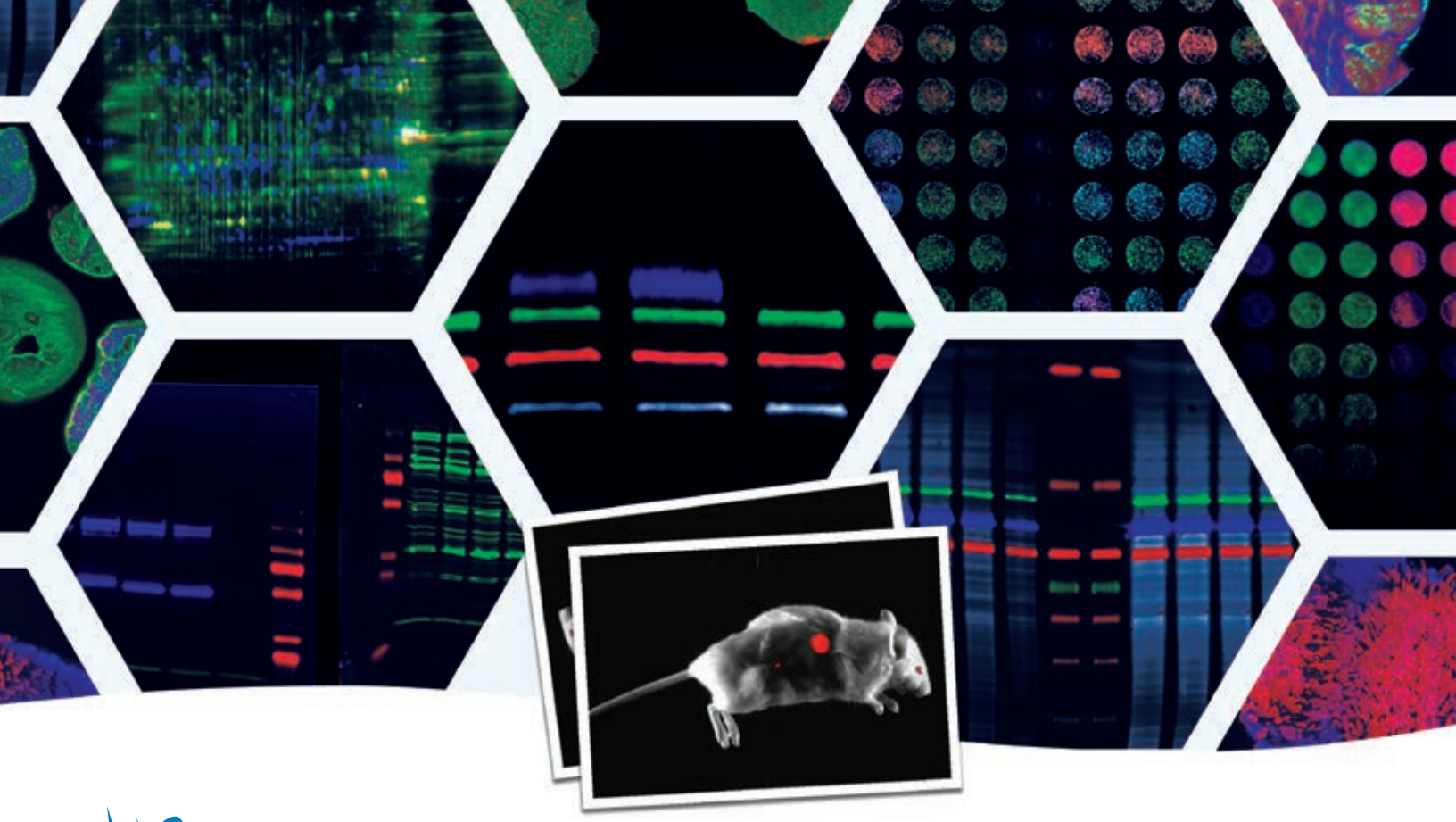

azure biosystems

Azure Sapphire™ FL Biomolecular Imager

UNLIMITED POSSIBILITIES, UNCOMPROMISING PERFORMANCE

Applications & Publications

TABLE OF CONTENTS

WESTERN BLOTS

cancers

Shikonin Reduces Growth of Docetaxel-Resistant Prostate Cancer Cells Mainly through Necroptosis

Sascha D. Markowitsch, Kira M. Juetter, Patricia Schupp, Kristine Hauschulte, Olesya Vakhrusheva, Kimberly Sue Slade, Anita Thomas, Igor Tsaur, Jindrich Cinatl, Jr., Martin Michaelis, Thomas Efferth, Axel Haferkamp and Eva Juengel

> "...To explore the expression and activity of cell cycle and cell death regulating proteins, Western blot analysis was performed...The membranes were incubated with ECL detection reagent (AC2204, Azure Biosystems, Munich, Germany) to visualize proteins with a Sapphire Imager (Azure Biosystems, Munich, Germany)...Cell death regulating proteins were normalized to total protein that was quantified by staining total protein from all membranes with Coomassie brilliant blue and measuring with a Sapphire Imager..."

Cancers. 2021;13(4):882

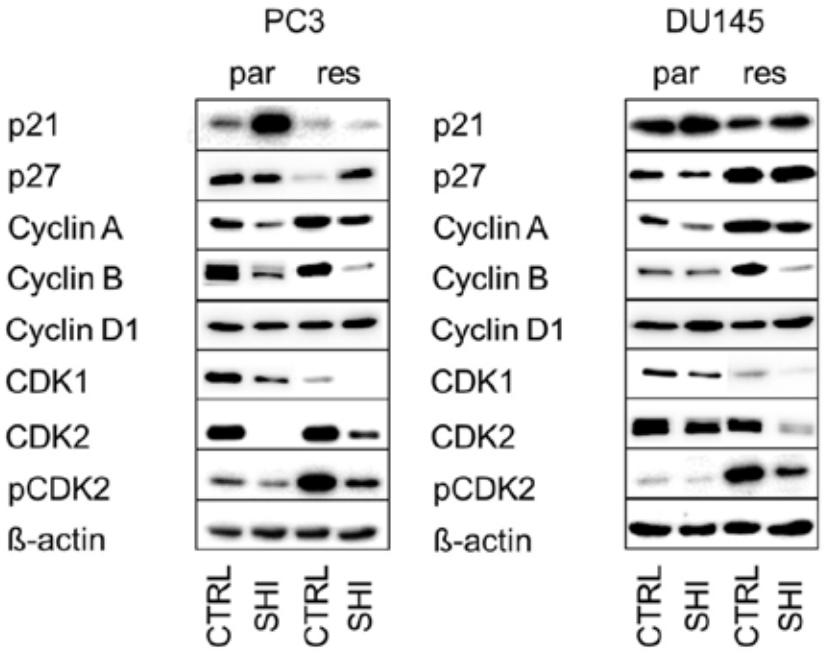

Figure 4. Protein expression profile of cell cycle regulating proteins: Representative Western blot images of cell cycle regulating proteins in parental (par) and DX-resistant (res) PC3 (left panel) and DU145 (right panel) cells after 48 h exposure to SHI [0.5 µM].

WESTERN BLOTS

frontiers in Immunology

NonO Is a Novel Co-factor of PRDM1 and Regulates Inflammatory Response in Monocyte Derived-Dendritic Cells

Kyungwoo Lee, Su Hwa Jang, Hong Tian and Sun Jung Kim

"...Proteins bound by antibody were visualized by ECL (Thermo Scientific, #34580 or Advansta, K-12045) and sapphire biomolecular imager (Azure Biosystems)..."

Front Immunol. 2020;11:1436

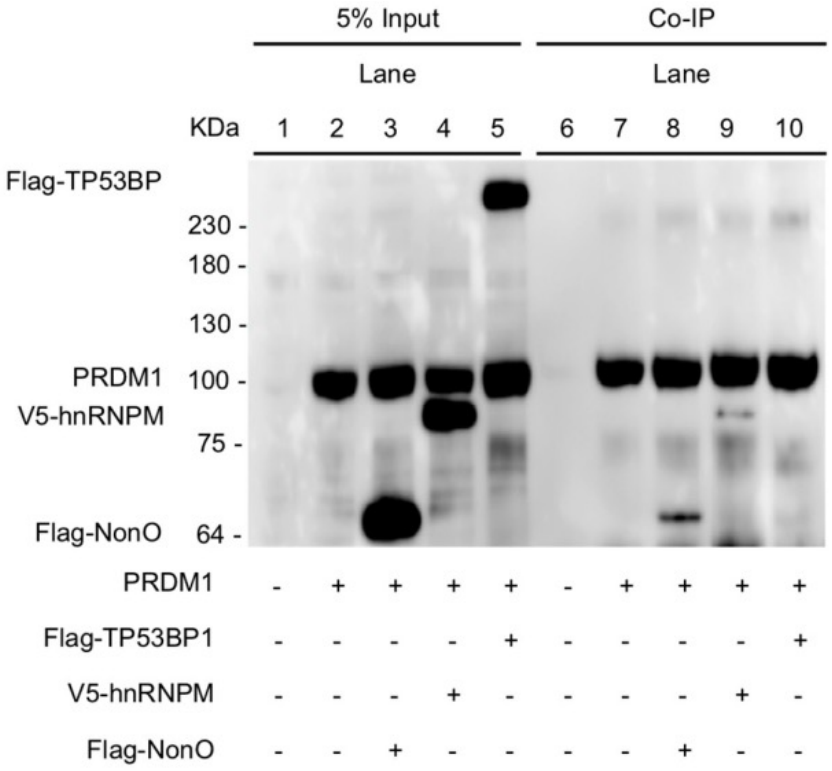

Figure 1(A). Nuclear fraction was immunoprecipitated with anti-PRDM1 antibodies and immunoblotting was performed with anti-PRDM1, Flag-NonO, Flag-TP53BP1, or V5-hnRNPM antibody. A representative image from two independent experiments is shown.

WESTERN BLOTS

Effects of prolactin on ventricular myocyte shortening and calcium transport in the streptozotocin-induced diabetic rat

Frank C. Howarth, Gunnar Norstedt, Oleksiy I. Boldyriev, Muhammad A. Qureshi, Ozaz Mohamed, Khatija Parekh, Balaji Venkataraman, Sandeep Subramanya, Anatoliy Shmygol, Lina T. Al Kury

"...The blots were developed using the Super Signal West Pico Plus chemiluminescent substrate (34577, Thermo Scientific, Rockford, IL, USA). The blot images were acquired using a Sapphire Biomolecular Imager (Azure Biosystems, Dublin, California, USA) using chemiluminescent detection of HRP, coupled with color image acquisition of the protein ladder..."

Heliyon. 2020;6(4):e03797

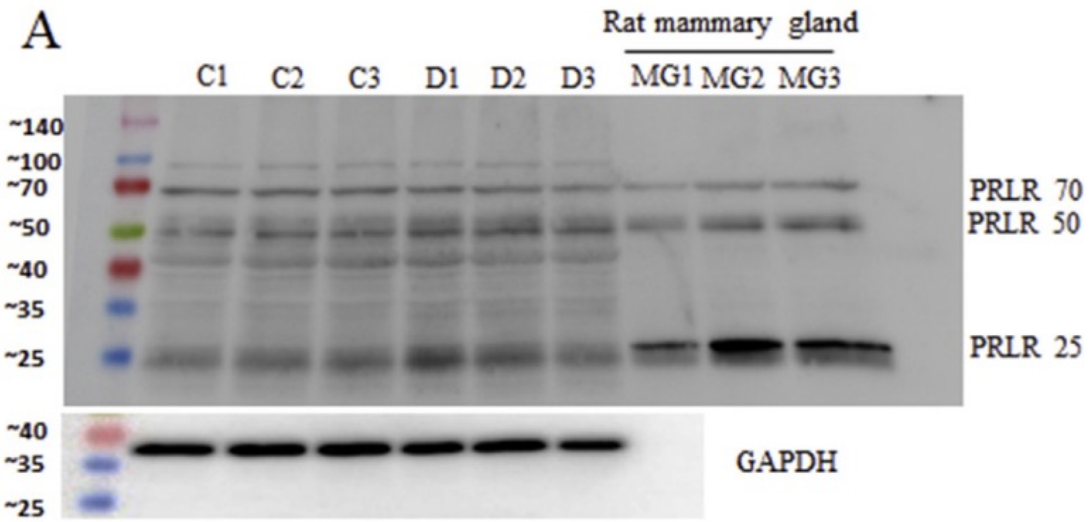

Figure 1. Expression of PRL receptor (PRLR) protein in ventricle tissue from STZ-induced diabetic and control hearts. Typical Western blots showing expression of PRLR protein in three control (C1 – C3) and 3 diabetic (D1-D3), GAPDH loading control and PRLR protein in tissue from 3 rat mammary glands (MG1-MG3) from 3 female rats, 5 days following delivery.

WESTERN BLOTS

Life Science Alliance

A dominant negative mitofusin causes mitochondrial perinuclear clusters because of aberrant tethering

Stephanie R Sloat, Suzanne Hoppins

"...Membranes were developed in Radiance Plus Chemiluminescent HRP Substrate (Azure Biosystems) for 5 min and imaged on a Sapphire Biomolecular Imager (Azure Biosystems). Band intensities were quantified using AzureSpot analysis software (Azure Biosystems)... Western blot images for shRNA were acquired on Sapphire, and quantification was performed with AzureSpot. Knockdown quantification was normalized using whole-protein stain (Azure Biosystems)"

Life Sci Alliance. 2022;6(1):e202101305

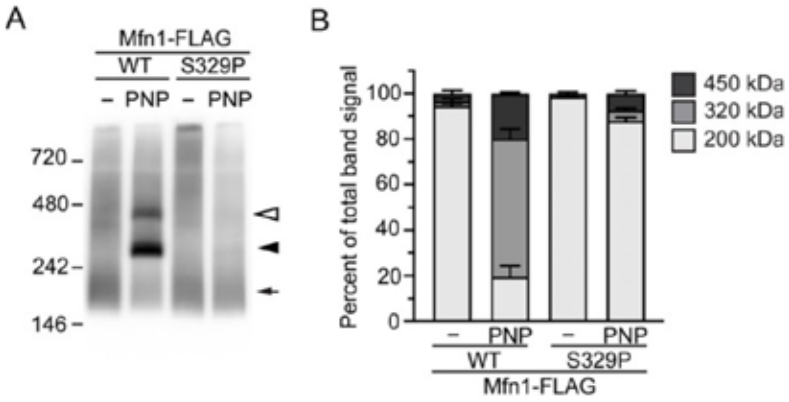

Figure 7. Mfn1^{S329P} is defective for GTP-dependent oligomerization. (A) Representative blue native–PAGE of mitochondria isolated from Flp-In TREx cells expressing Mfn1^{WT}-FLAG or Mfn1^{S329P}-FLAG after incubation with 0.2 μg/ml TET for 4 h. Mitochondria were untreated or incubated in the presence of GMP-PNP (PNP), followed by solubilization and separation by blue native–PAGE and immunoblotted with α-FLAG. Arrow indicates ~200-kD species, closed arrowhead indicates ~320-kD species, and open arrowhead indicates ~450-kD species. Molecular-weight markers are indicated in kD on left. (A, B) Quantification of native mitofusin species indicated in A. Error bars represent mean ± SEM from n = 3 separate experiments.

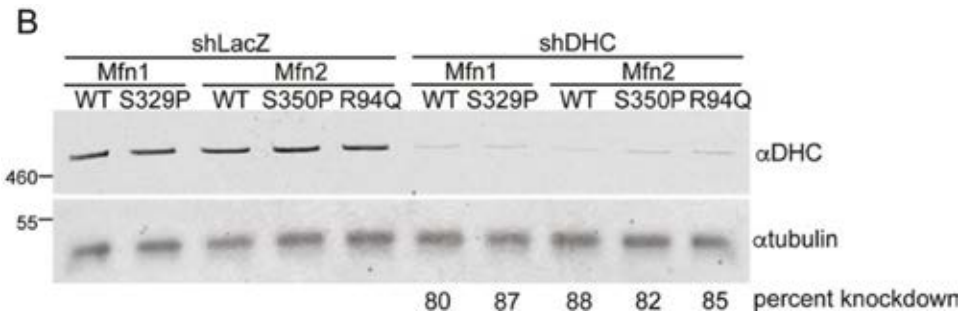

Supplemental Figure 6B. Representative Western blot of α-DHC and α-tubulin in whole-protein extract from cells treated with either control shRNA (shLacZ) or shRNA against DHC (shDHC). Molecular-weight markers are indicated in kD on left. Percent knockdown represents mean knockdown of DHC n = 3 quantified by band intensities in Western blot normalized to whole-protein stain.

PROTEIN ARRAYS

frontiers in Cell and Developmental Biology

In vitro Evaluation of ASCs and HUVECs Co-cultures in 3D Biodegradable Hydrogels on Neurite Outgrowth and Vascular Organization

Luís A. Rocha, Eduardo D. Gomes, João L. Afonso, Sara Granja, Fatima Baltazar, Nuno A. Silva, Molly S. Shoichet, Rui A. Sousa, David A. Learmonth and Antonio J. Salgado

> "...The evaluation of the angiogenic and neurotrophic profile of the previously obtained secretomes was performed using the Human Neuro Discovery Array C1 and Human Angiogenesis Array C1 (RayBiotech, United States)...Finally, the chemiluminescence image of each membrane was obtained using a Sapphire Biomolecular Imager (Azure Biosystems, United States). The intensity of each dot was quantified using the AzureSpot software (Azure Biosystems, United States)..."

Front Cell Dev Biol. 2020;8:489

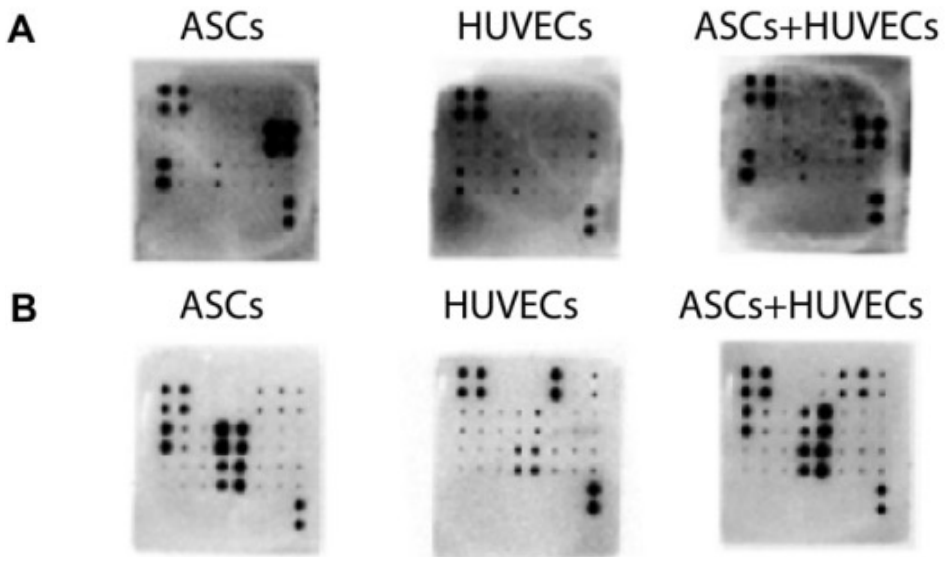

Figure 5. Analysis of the secretomes of ASCs, HUVECs, and their co-culture after 7 days of culture in GG-GRGDS allowed to understand the relative expression of a panel of neuroregulatory and angiotrophic molecules. (A) The secretome of ASCs+HUVECs showed an upregulation on different neurotrophic factors (BDNF, β-NGF, IGF-1, and S-100 B) showing a positive effect of the interaction of both cells on the secretion of these molecules.

PLANT LEAF BIOLUMINESCENCE

nature plants

A species-specific functional module controls formation of pollen apertures

Byung Ha Lee, Rui Wang, Ingrid M. Moberg, Sarah H. Reeder, Prativa Amom, Michelle H. Tan, Katelyn Amstutz, Pallavi Chandna, Adam Helton, Ekaterina P. Andrianova, Igor B. Zhulin, and Anna A. Dobritsa

> “Agrobacteria were collected and resuspended in infiltration buffer (10 mM MgCl2, 10 mM MES, 150 μM acetosyringone) at a final concentration of OD600 = 0.8. Pairwise combinations of suspensions were infiltrated into young tobacco leaves, which were then allowed to grow for 3 d in light. A total 12–16 leaves were collected from five to ten plants, the abaxial side of leaves was sprayed with 1 mM luciferin (Biosynth, L-8220) and kept in the dark at 4 °C for 30 min. The bioluminescence images were captured using Azure Sapphire Biomolecule Imager (Azure Biosystems) and converted to heatmaps using the 16-colour look-up table from ImageJ v.1.53a...”

Nat Plants. 2021;7(7):966-978

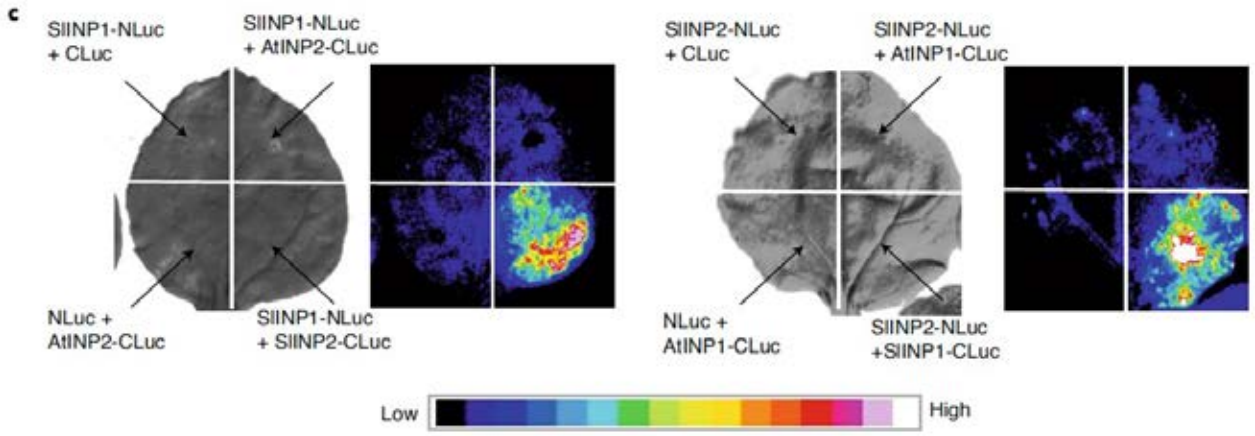

Figure 6c. Split-luciferase assay testing the ability of SlINP1 and SlINP2 to interact. Tobacco leaves were divided into sectors co-expressing indicated proteins containing the N-terminal (NLuc) and C-terminal (CLuc) parts of the firefly luciferase. Panels on the left show the bright-field images and panels on the right show the corresponding luminescence images. Split-luciferase assay testing the ability of INP1 and INP2 from Arabidopsis and tomato to interact with a protein from another species. Only the same-species interactions were observed.

WESTERN BLOTS

Chemical Science

Engineered unnatural ubiquitin for optimal detection of deubiquitinating enzymes

Wioletta Rut, Mikolaj Zmudzinski, Scott J. Snipas, Miklos Bekes, Tony T. Huang and Marcin Drag

> “...Biotinylated Ub-based probes were detected with a fluorescent streptavidin Alexa Fluor 647 conjugate (1 : 10 000) in TBS-T with 1% BSA, and UCH-L3 was detected with a mouse anti-human monoclonal IgG1 antibody (1 : 1000) and fluorescent goat anti-mouse (1 : 10 000) using an Azure Biosystems Sapphire Biomolecular Imager and Azure Spot Analysis Software.”

Chem Sci. 2020;11(23):6058-6069

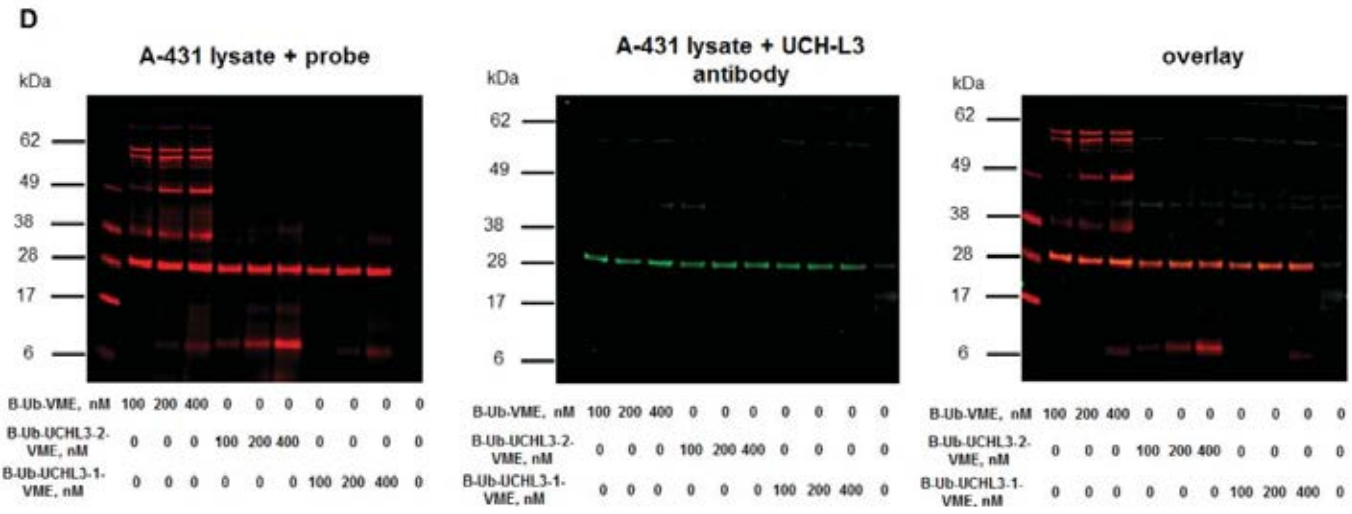

Figure 5(D). Detection of UCH-L3 in A-431 cell lysates using Ub-based probes (using a streptavidin Alexa Fluor 647 conjugate) and a UCH-L3 antibody.

IN-GEL IMAGING

Chemical Science

Parallel imaging of coagulation pathway proteases activated protein C, thrombin, and factor Xa in human plasma

Sylwia Modrzycka, Sonia Kołt, Stéphanie G. I. Polderdijk, Ty E. Adams, Stanisław Potoczek, James A. Huntington, Paulina Kasperkiewicz and Marcin Drąg

> “...For the simultaneous coagulation factor labeling, human plasma was incubated with 5 μM of each fluorescently labeled probe...and then 5 μL of each sample was run onto a 10% MES (w/v) 15-well gel...The gel was then directly scanned at 520 nm for Cy3, 658 nm for Cy5, and 784 nm for Cy7 detection using an Azure Biosystems Sapphire Biomolecular Imager and Azure Spot Analysis Software.”

Chem Sci. 2022;13(23):6813-6029

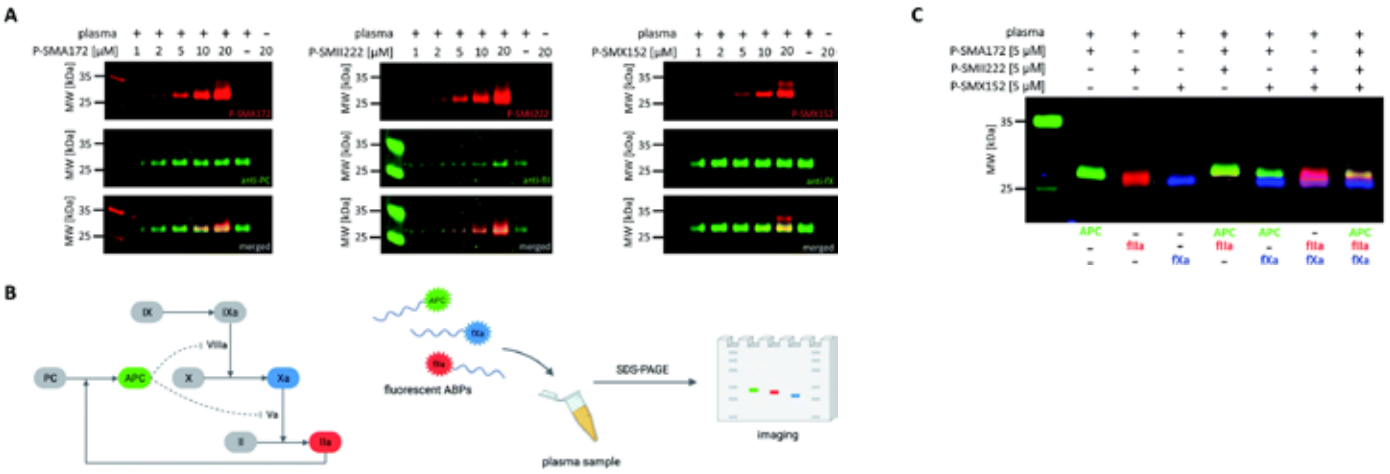

Figure 6. Coagulation factor (APC, thrombin, fXa) labeling in human plasma. (A) Probe concentration optimization assay. Human plasma was incubated with each fluorescent ABP separately at various probe concentrations ranging from 1 to 20 μM for 60 min at 37 °C. The samples were then subjected to SDS–PAGE analysis, transferred to a membrane, immunostained with the appropriate antibody, and imaged using an Azure Biosystems Sapphire Biomolecular Imager as follows: for APC at 658 nm (for Cy5 detection) and 488 nm (for antibody detection), for thrombin at 784 nm (for Cy7 detection) and 658 nm (for antibody detection), for fXa at 520 nm (for Cy3 detection) and 658 nm (for antibody detection). The results are representative of at least 3 replicates. (B) Graphical scheme of the methodology used for simultaneous coagulation factor detection in human plasma. (C) Simultaneous coagulation factor labeling in human plasma. Human plasma was incubated with 5 μM of each fluorescently labeled ABP and subjected to SDS–PAGE analysis. Direct in-gel analysis was performed with lasers of 520 nm for Cy3, 658 nm for Cy5, and 784 nm for Cy7 using an Azure Biosystems Sapphire Biomolecular Imager. The results are representative of at least 3 replicates.

LATERAL FLOW ASSAY DEVELOPMENT

Method for the elucidation of LAMP products captured on lateral flow strips in a point of care test for HPV 16

Lena Landaverde, Winnie Wong, Gabriela Hernandez, Andy Fan & Catherine Klapperich

> “...To identify 5'-FAM-specific LAMP products, unstained agarose and acrylamide gels were imaged under 488-nm laser excitation using the Sapphire Biomolecular Imager...”

Anal Bioanal Chem. 2020;412(24):6199-8209

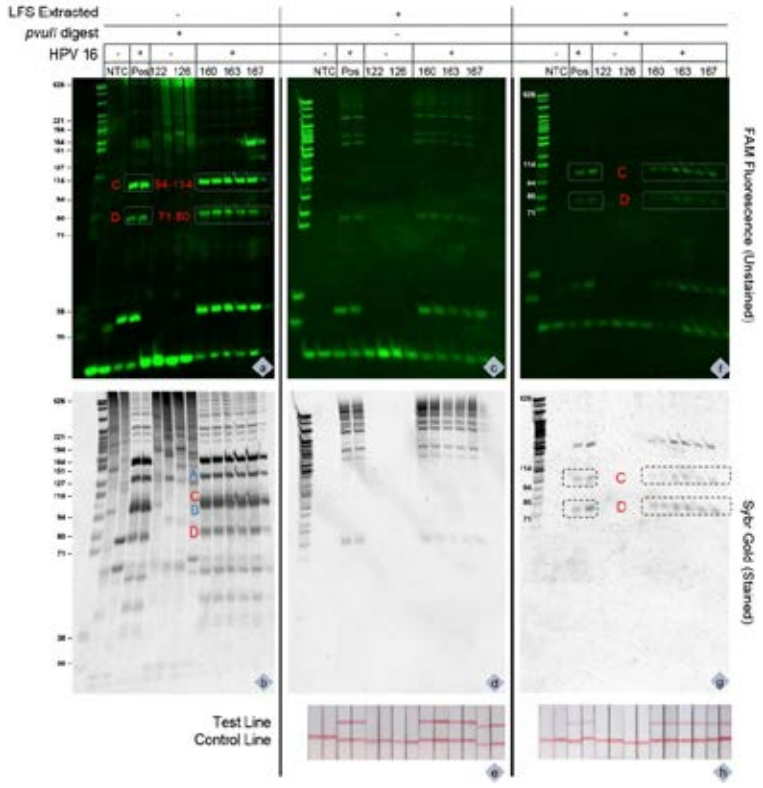

Figure 4. FAM band comparisons of *pvuII*-digested and undigested lateral flow strip elutions. Three different representations of the LAMP amplicon products are shown. Gel a and b are LAMP amplicons digested with *pvuII* (independent of LFS). Gels c, d, f, and g are eluted products from the LFS itself. Furthermore, gels c and d contain uncleaved LFS-LAMP products (*pvuII*–), whereas gels f and g are cleaved LFS-LAMP products (*pvuII*+). The FAM bands 94–114 (band C) bp and 71–80 bp (b and D) are highlighted as the HPV 16 FAM amplicons. Gel b also shows the previously sequenced bands of 146 (band A) and 92 (band B). The LFS strips that DNA was eluted from are shown in LFS images e and h of Fig. 4. The gels in panels a and b are *pvuII*-digested LAMP products; the lateral flow strips results are equivalent to the LFS shown in panel h.

2D DIGE

Proteomic Analysis of Endometrial Cancer Tissues from Patients with Type 2 Diabetes Mellitus

Muhammad Mujammami, Mohamed Rafiullah, Assim A. Alfadda, Khalid Akkour, Ibrahim O. Alanazi, Afshan Masood, Mohthash Musambil, Hani Alhalal, Maria Arafah, Anas M. Abdel Rahman and Hicham Benabdelkamel

"...The gels were scanned with Sapphire Biomolecular Imager (Azure Biosystems...) and digitalized via the image analysis software Sapphire Capture system (Azure Biosystems..."

Life.12(4):491

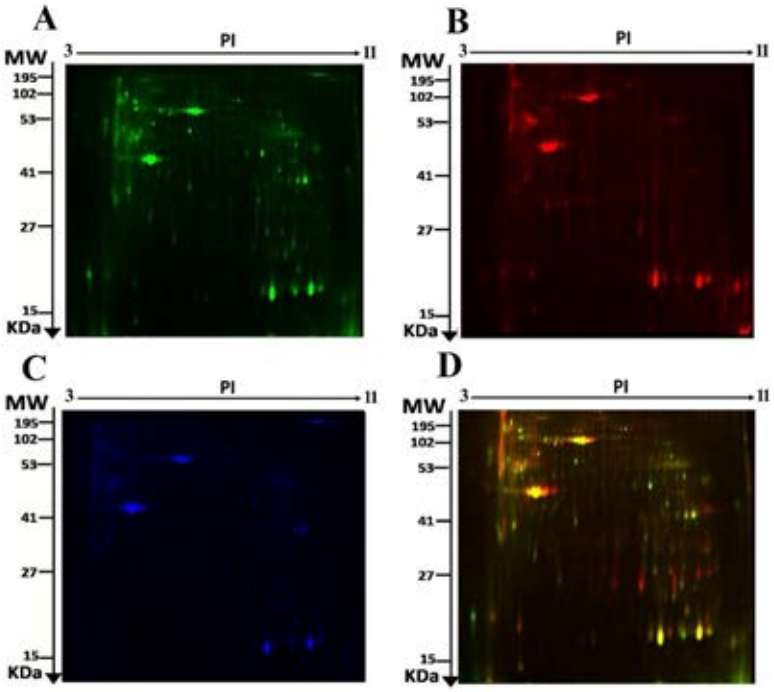

Figure 1. The representative fluorescent protein of a two-dimensional difference in gel electrophoresis (2D-DIGE) containing tissue samples from EC Diabetic samples labeled with Cy3 (A), EC Non-Diabetic samples labeled with Cy5 (B), pooled internal control labeled with Cy2 (C), and merged image (D).

GEL SHIFT ASSAY
(example of DNA-Protein Binding Assay)

Structure of a RecT/Redβ family recombinase in complex with a duplex intermediate of DNA annealing

Brian J. Caldwell, Andrew S. Norris, Caroline F. Karbowski, Alyssa M. Wiegand, Vicki H. Wysocki & Charles E. Bell

> “...A gel shift DNA binding assay used two complementary 50-mer oligonucleotides labeled at the 5'-end with either Cy3 or Cy5...For visualization 17.5 µl of each complex was mixed with 7.5 µl Orange G dye...Gels were imaged using a Sapphire Biomolecular Imager (Azure Biosystems) with Sapphire Capture Software (version 1.12.0921.0). Scanning parameters for Fig. 8 were pixel size 100 µm, scan speed high, 2.38mm focus, intensity 2 for Cy5, intensity 4 for Cy3, black lighting 50, white 37186, gamma 1.37. Scanning parameters for Supplementary Fig. 1a, b were intensity 1 for Cy5, intensity 2 for Cy3, black lighting 50, white 15362, gamma 0.88.”

Nat Commun. 2022;13(1):7855

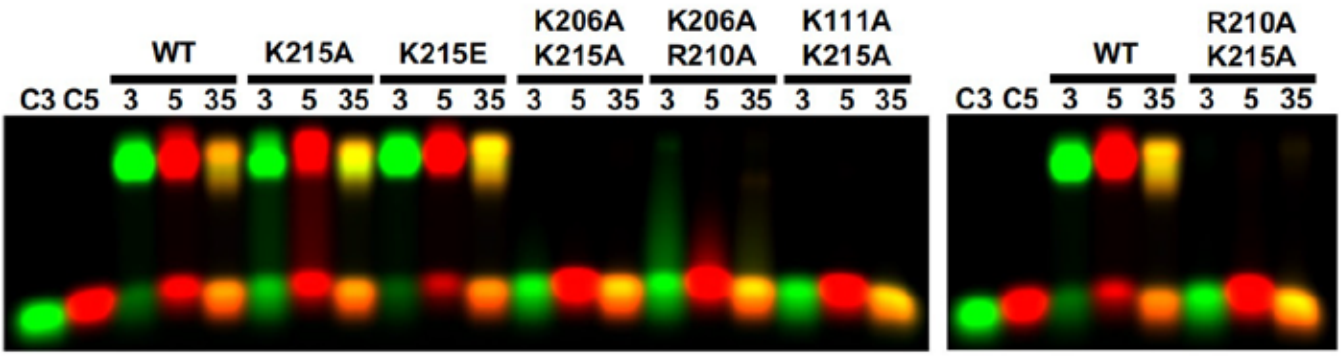

Figure 8 (a). Mutational analysis. Each panel shows a gel-shift assay with 3.6 µM of LiRecT mixed with different combinations of Cy3- and Cy5-labeled 50mer oligonucleotides (25 µM nucleotides). Lanes C3, C5: each oligo without protein. Lanes 3, 5: LiRecT mixed with each individual oligonucleotide (Cy3-50mer or Cy5-50mer) to form a ssDNA complex. Lanes 35: LiRecT incubated with Cy3- 50mer at 37° for 15 min, followed by addition of Cy5-50mer and incubation for an additional 15 min to form the duplex intermediate (yellow band).

ORGAN IMAGING

Visible Fluorescence

nature cardiovascular research

Neutrophils incite and macrophages avert electrical storm after myocardial infarction

Jana Grune, Andrew J. M. Lewis, Masahiro Yamazoe, Maarten Hulsmans, David Rohde, Ling Xiao, Shuang Zhang, Christiane Ott, David M. Calcagno, Yirong Zhou, Kerstin Timm, Mayooran Shanmuganathan, Fadi E. Pulous, Maximilian J. Schloss, Brody H. Foy, Diane Capen, Claudio Vinegoni, Gregory R. Wojtkiewicz, Yoshiko Iwamoto, Tilman Grune, Dennis Brown, John Higgins, Vanessa M. Ferreira, Neil Herring, Keith M. Channon, Stefan Neubauer, Oxford Acute Myocardial Infarction (OxAMI) Study,* David E. Sosnovik, David J. Milan, Filip K. Swirski, Kevin R. King, Aaron D. Aguirre, Patrick T. Ellinor, and Matthias Nahrendorf

> “...Oxidative stress was imaged after intravenous injection of CellROX Deep Red Reagent (C10422, Thermo Fisher Scientific, 20 µl diluted in 100 µl of PBS). Hearts were sliced in 1-mm sections for immediate imaging using a Sapphire Biomolecular Imager (Azure Biosystems)...”

Nat Cardiovasc Res. 2022;1(7):649–664

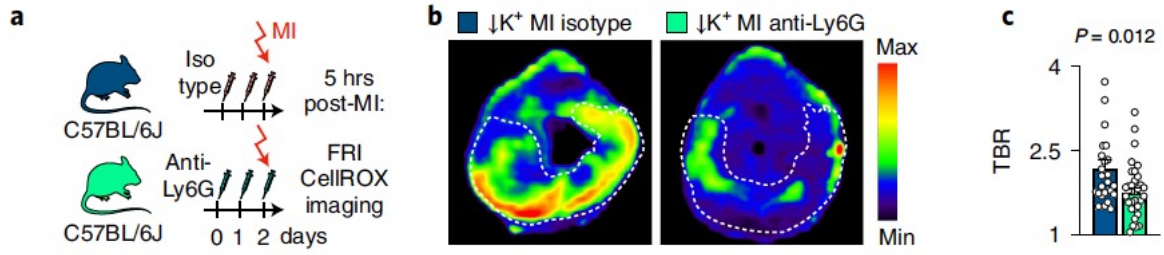

Figure 3a. Experimental outline. FRI of ROS in hearts 5 hours after MI using the CellROX imaging agent. b, Fluorescence images from cardiac short axis slices after injection of CellROX. c, Quantification of TBR from FRI. Data are from isotype antibody-injected controls (n = 6 mice) and neutrophil-depleted mice (n = 7). Each dot represents a cardiac slice.

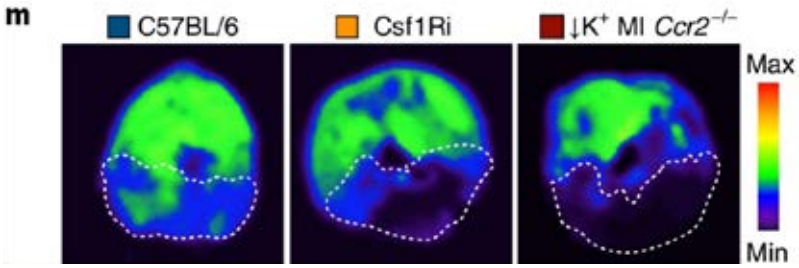

Figure 6m. Representative images of TMRE imaging.

Abbreviations: FRI, fluorescence reflectance imaging; MI, myocardial infarction; ROS, reactive oxygen species; TBR, target-to-background ratio

TUMOR IMAGING

Visible Fluorescence

Molecular Therapy
Oncolytics

Eliminating mesothelioma by AAV-vectored, PD1-based vaccination in the tumor microenvironment

Zhiwu Tan, Mei Sum Chiu, Chi Wing Yan, Kwan Man, Zhiwei Chen

"...resected REN tumor fluorescence was imaged with a Sapphire Biomolecular Imager (Azure Biosystems) after surgical resection..."

Mol Ther Oncolytics. 2021;20:373–386

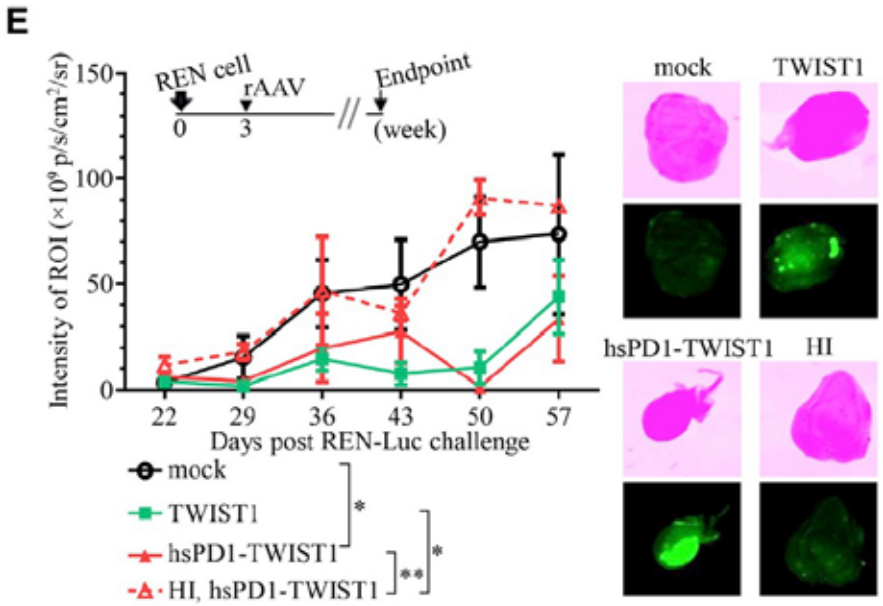

Figure 5. Localized injection of rAAV-hsPD1-TWIST1 inhibits human mesothelioma in NSG-huPBL mice. (E) REN tumors in NSG mice (n = 4). 2 x10^6 REN cells were injected s.c. into NSG mice 3 weeks before i.t. administration of 5 x 10^{11} g.c. rAAV. Left: tumor growth was measured by bioluminescence imaging. Right: representative tumor fluorescence images at the endpoint. Mock, PBS treatment.

MODIFIED MICROPLATES

ADVANCED MATERIALS INTERFACES

ZnO Nanowire-Based Early Detection of SARS-CoV-2 Antibody Responses in Asymptomatic Patients with COVID-19

Jung Kim, Sung Kyun Lee, Jong-Hwan Lee, Hye-Yeon Kim, Nam Hoon Kim, Chang Hoon Lee, Chang-Seop Lee, and Hong Gi Kim

> “...NP antigen in coating buffer A (CB07100, Invitrogen, USA) was prepared at 1, 3, or 5 μg mL−1 and added to the ZnO-NW MP. Next, the anti-NP polyclonal antibody (32, 160, or 800 ng mL−1) in assay buffer (DS98200, Invitrogen, USA) was applied to the plate for 1 h, followed by the Alexa Fluor 488-conjugated secondary antibody (A-11034; 1 mg mL−1) for a further hour. The plate was washed between these steps. The fluorescence signal was measured in a microplate reader and a image taken under a laser scanning imager (Sapphire Biomolecular Imager, Azure biosystems, USA)...”

Adv Mater Interfaces. 2022;9(14):2102046

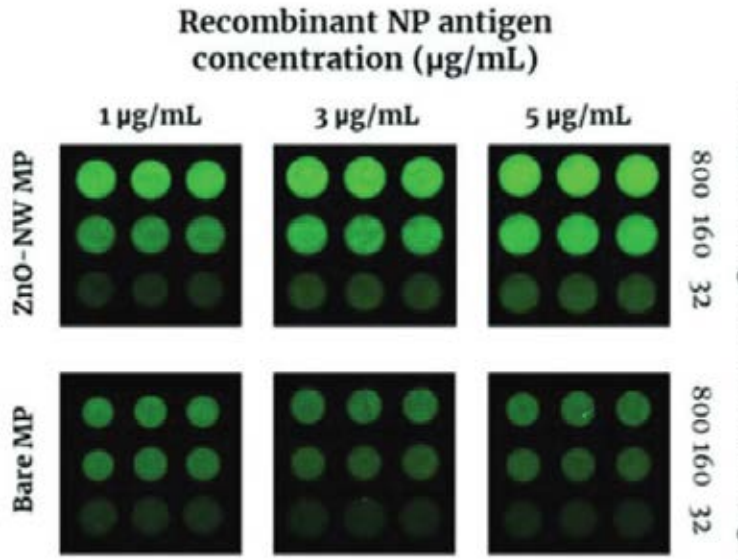

Figure 2 (b). Introduction of SARS-CoV-2 NP antigen onto the surface of the ZnO-NW MP, and detection of anti-SARS-CoV-2 NP IgG polyclonal antibodies. SARS-CoV-2 NP antigen (1, 3, or 5 μg mL−1) was coated onto the ZnO-NW MP and bare MP. Measurement of the bound rabbit anti- SARS-CoV-2 NP IgG polyclonal antibody (32, 160, or 800 ng mL−1) using anti-human IgG conjugated to Alexa 488.

Abbreviations: MP, microplate; NP, nucleocapsid; NW, nanowire.

TISSUE IMAGING

White Light and Autofluorescence

ANIMAL MODELS AND EXPERIMENTAL MEDICINE

Rescue of autoimmune hepatitis by soluble MHC class II molecules in an altered concanavalin A-induced experimental model

Katerina Bakela, Maria Georgia Dimitraki, Evangelia Skoufa, Irene Athanassakis

"...Liver tissues were isolated 6 months after the ConA and the ConA + sMHCII treatment of mice and fixed using PFA 4%, under rotation, at 4°C for 24 hours. Azure Biosystems Sapphire™ Biomolecular Imager (Azure Biosystems, Dublin, CA 94568 USA) was used in order to scan the liver tissues in 10-μm resolution. This instrument combines NIR fluorescence (both long and short), RGB fluorescence, chemiluminescent, and phosphor imaging capabilities, while using four solid state lasers as excitation sources (450, 520, 660, and 780 nm). The application of the four-channel fluorescence mode at 10-μm resolution, could detect gross anatomy and morphology of liver tissues, mainly based on tissue autofluorescence..."

Animal Model Exp Med. 2020;3(3):264–272

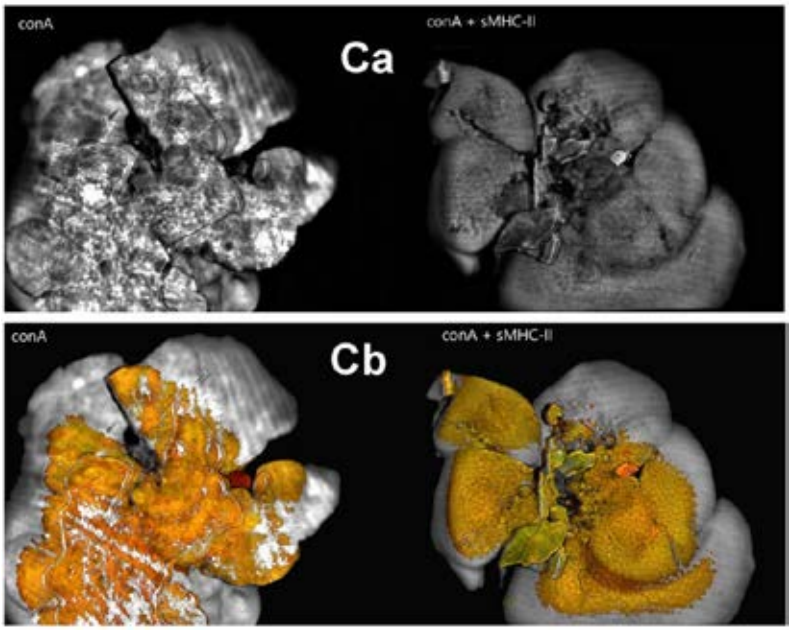

Figure 6. Livers were isolated, fixed and scanned using a white light beam at 10-μm resolution (Ca) or four-channel fluorescence at 10-μm resolution (Cb).

WESTERN BLOTS

Accumulation and persistence of ivacaftor in airway epithelia with prolonged treatment

Tara N. Guhr Lee, Deborah M. Cholon, Nancy L. Quinney, Martina Gentzsch, Charles R. Esther Jr

> “...Blots were probed with mouse monoclonal anti-CFTR antibodies and then with IRDye 680–goat anti-mouse immunoglobulin G (Molecular Probes). Anti-actin (Cell Signaling) was used as a loading control. Protein bands were visualized using a Sapphire Biomolecular Imager (Azure Biosystems)...”

J Cyst Fibros. 2020;19(5):746-751

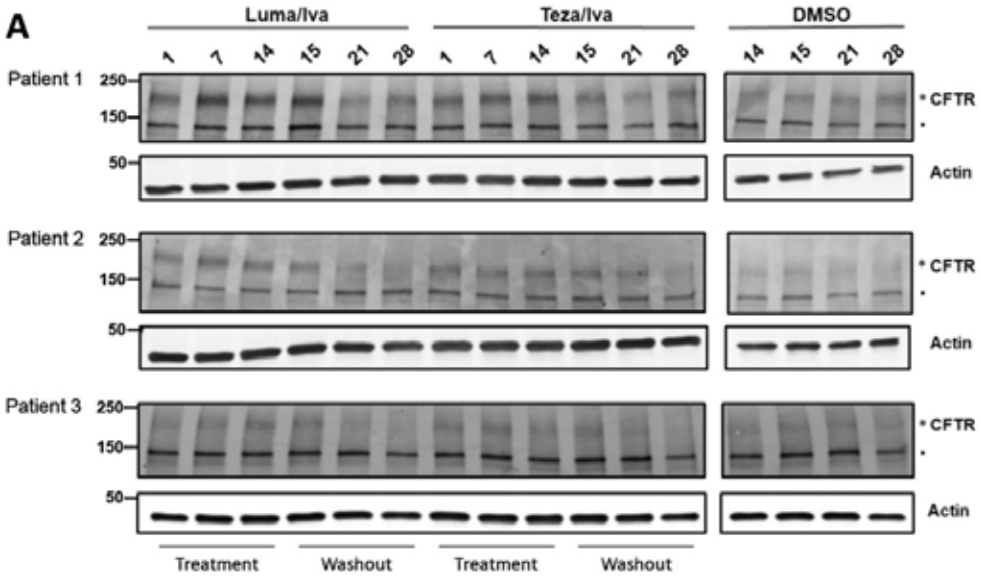

Fig. 3 (A). Mature CFTR protein (band C, ⁎) and immature CFTR protein (band B, •) visualized by Western blot analysis of HBE cultures derived from 3 CF (F508del/F508del) patients. Numbers at the top of the lanes represent days since treatment start. Actin is shown as a loading control.

WESTERN BLOTS

CONTACT DERMATITIS
CUTANEOUS ALLERGY
ENVIRONMENTAL AND OCCUPATIONAL DERMATITIS

Differential influence of Streptococcus mitis on host response to metals in reconstructed human skin and oral mucosa

Lin Shang, Dongmei Deng, Sanne Roffel, and Susan Gibbs

"...membranes were washed three times in PBST and further incubated with infrared dye-conjugated secondary antibodies against mouse (1:7500 for TLR3, 4, or 5) or against rabbit (1:7500 for TLR1, 2, 6, or tubulin). After washing, the blots were visualized using Sapphire Biomolecular Imager (Azure biosystems, Dublin, California)..."

Contact Dermatitis. 2020;83(5):347–360

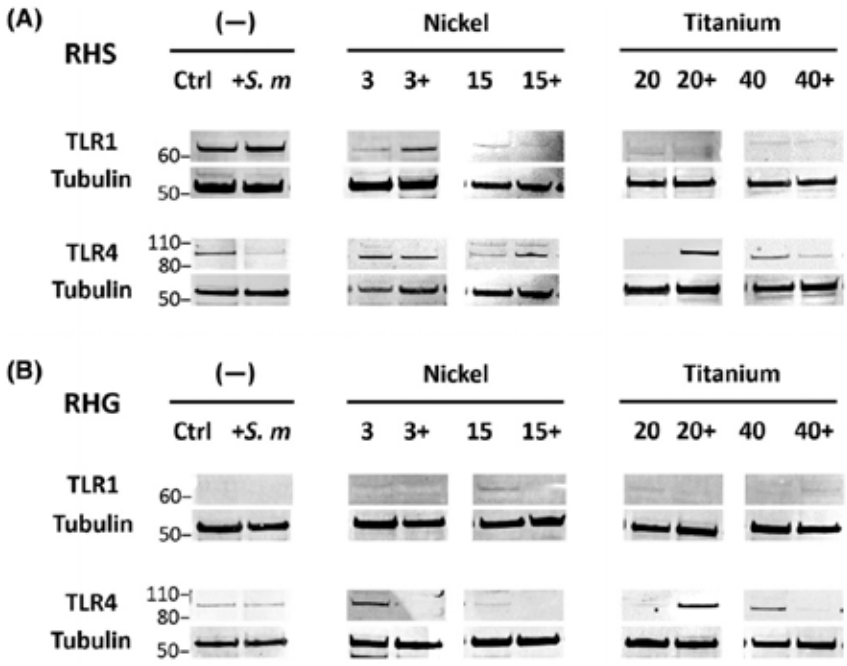

Figure 6. Toll-like receptor (TLR) protein expression in reconstructed human skin (RHS) and gingiva (RHG). TLR1 and 4 proteins are shown together with reference tubulin expression. TLR2, 3, 5, and 6 were under the detectable level (data now shown). Data are representative of three independent experiments.

IN-CELL WESTERN

Alboserpin, the Main Salivary Anticoagulant from the Disease Vector Aedes albopictus, Displays Anti–FXa-PAR Signaling In Vitro and In Vivo

Gaurav Shrivastava, Paola Carolina Valenzuela-Leon, Andrezza Campos Chagas, Olivia Kern, Karina Botello, Yixiang Zhang, Ines Martin-Martin, Markus Berger Oliveira, Lucas Tirloni, and Eric Calvo

"...Finally, the plates were scanned at 700 and 800 nm, and the intensity of the labeled proteins was measured using the Azure sapphire biomolecular imager (Azure Biosystems)"

Immunohorizons.2022;6(6):373–383

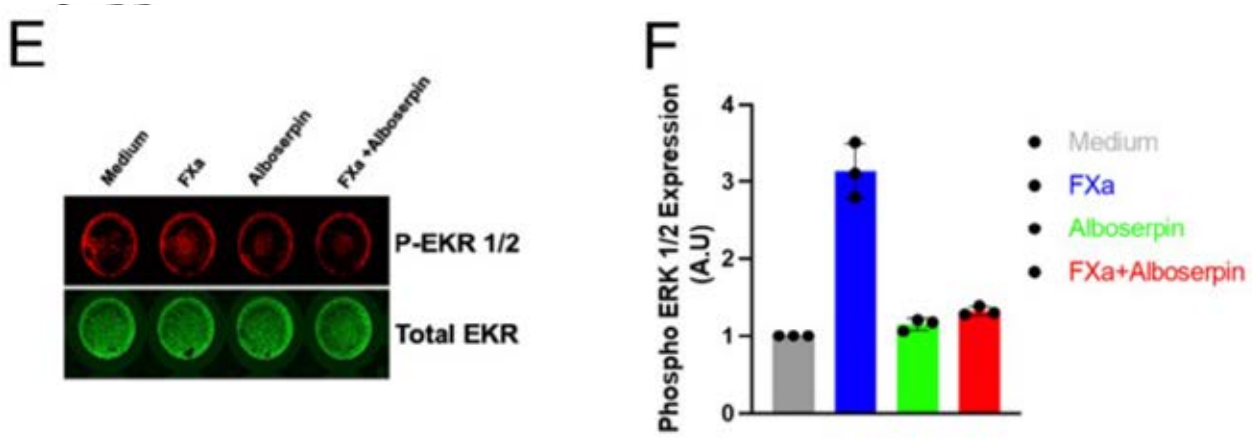

Figure 1. Alboserpin inhibits FXa inflammatory effect in vitro. ...(E) ERK1/2 protein expression was analyzed using In- Cell Western blots (ICW). (F) Intensity ratio (p-ERK/ERK).

MOBILITY SHIFT ASSAYS

High Dose IFN-β Activates GAF to Enhance Expression of ISGF3 Target Genes in MLE12 Epithelial Cells

Kensei Kishimoto, Catera L. Wilder, Justin Buchanan, Minh Nguyen, Chidera Okeke, Alexander Hoffmann and Quen J. Cheng

> "...Nuclear extracts...were incubated with P32-labaled oligonucleotide probes...The reaction mixtures were run on a 5% acrylamide (30:0.8) gel with 5% glycerol and TGE buffer (24.8 mM Tris, 190 mM glycine, 1 mM EDTA) at 200V for 1 hour and 45 mins. The gels were dried and imaged on a Sapphire Biomolecular imager in phosphor mode (Azure Biosystems, Dublin, CA)."

Front Immunol. 2021;12:651254

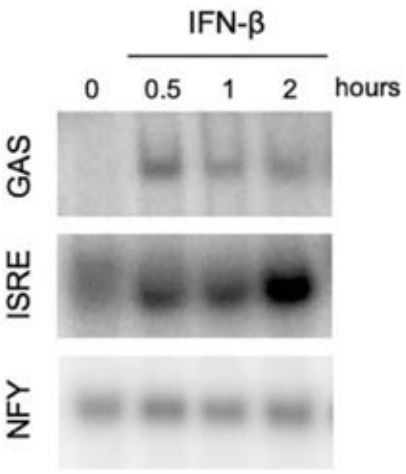

Figure 1. IFN-β Induced STAT1 binds to GAS and ISRE motifs. (A) EMSA of GAS and ISRE binding in MLE12 cells treated with IFN-β (100 U/ml). NFY shown as loading control. Data are representative of >5 independent experiments.

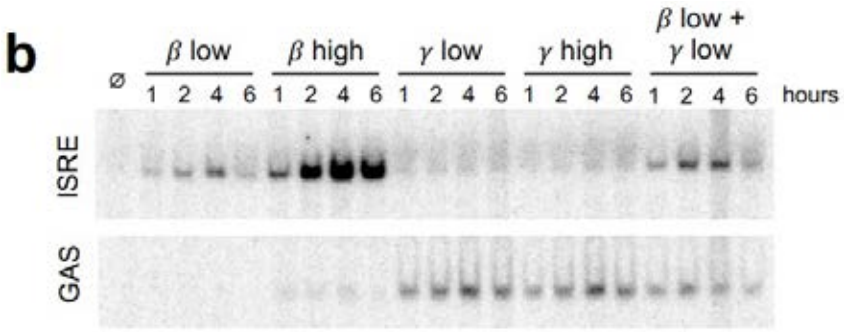

Figure 5. EMSA of ISRE and GAS binding in response to IFN-β (1 vs.100 U/mll), IFN-γ (1 vs.100 ng/ml), or a mixture of the low doses. Representative gel from five replicates.

RNA GELS

Engineered Viral RNA Decay Intermediates to Assess XRN1-mediated decay

Joseph Russo, Cary T. Mundell, Phillida A. Charley, Carol Wilusz, and Jeffrey Wilusz

> “...The samples were then resolved via denaturing PAGE, dried, exposed to a phosphor screen, and viewed via an Azure Sapphire Biomolecular Imager providing sufficient sensitivity to observe all required bands with one exposure.”

Methods. 2019;155:116–123

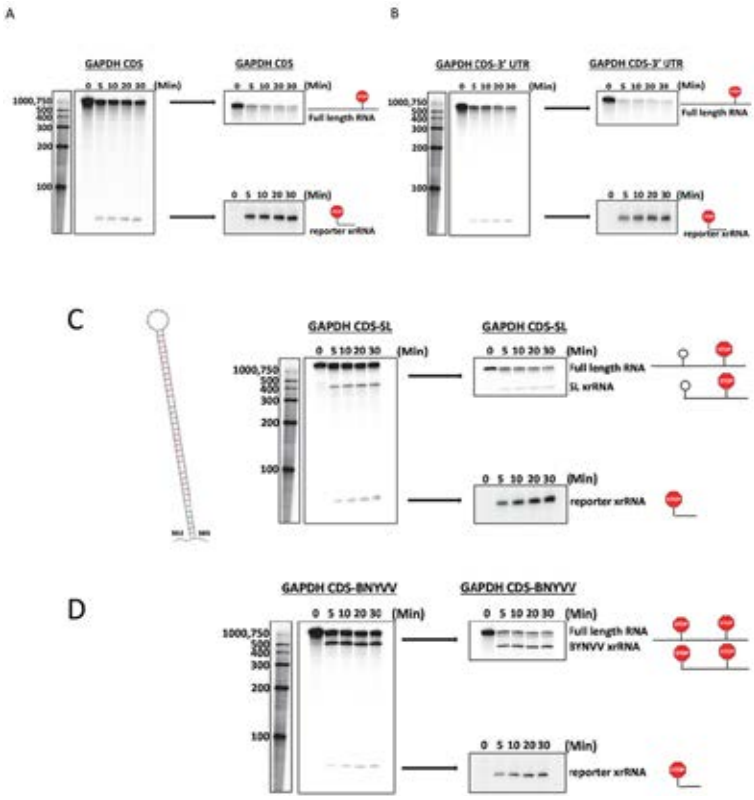

Figure 3. *In vitro* decay assay and xrRNA read-out using different RNA substrates.

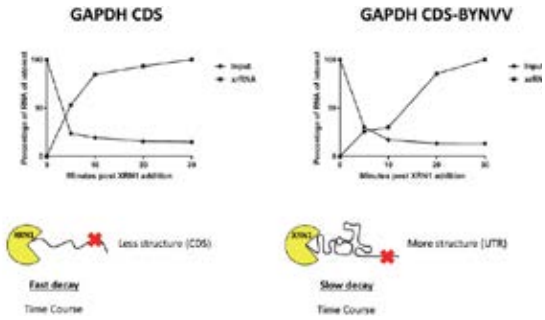

Figure 4. Quantification/graphical representation of gels presented in vitro decay assays and xrRNA readouts of selected RNA substrates. Using the representative data obtained in Fig. 3, the relative levels of the full length input RNA (Input circles) or the xrRNA reporter decay intermediate (xrRNA squares) for GAPDH CDS and GAPDH CDS-BNYVV were quantified by phosphorimaging using pixel counting. Results are presented as the amount of the indicated RNA species relative to the band/lane of the gel with the maximal pixel count for each RNA.

SOUTHERN BLOTS

PLOS PATHOGENS

Host cell-dependent late entry step as determinant of hepatitis B virus infection

Xupeng Hong, Yuka Imamura Kawasawa, Stephan Menne, Jianming Hu

"...Viral DNAs were resolved on 1.2% agarose gel and detected by 32P-labeled HBV or WHV DNA probes...DNA signals from Southern blot analysis were detected by Sapphire Biomolecular Imager (Azure Biosystems) and quantified using the Image Lab system 6.0.1 (Bio-Rad)."

PLoS Pathog. 2022;18(6):e1010633

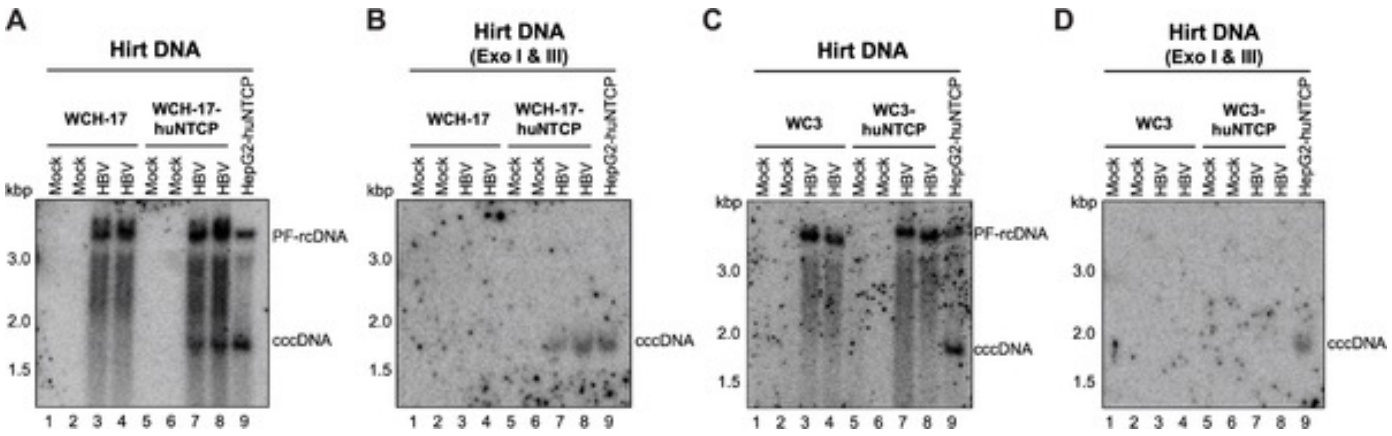

Figure 4. WCH-17 cells were rendered susceptible to HBV infection after huNTCP expression. WCH-17 (A, B) or WC3 (C, D) parental and huNTCP-expressing cells were plated on regular culture dishes (i.e., with no collagen coating) and infected with ca. 400 genome equivalent of HBV per cell. Three days post infection, the PF DNA (i.e., Hirt DNA) from mock- or HBV-infected cells was extracted by Hirt extraction and treated with Exo I/III followed by Southern blot analysis. Hirt DNA from HBV-infected HepG2-huNTCP cells, loaded at 4-fold less than the Hirt DNA from woodchuck cells, served as the positive control for cccDNA detection.

TISSUES

Preclinical evaluation of [^{18}F]FDG- PET as a biomarker of lymphoid tissue disease and inflammation in Zika virus infection

Carla Bianca Luena Victorio, Joanne Ong, Jing Yang Tham, Marie Jennifer Reolo, Wisna Novera, Rasha Msallam, Satoru Watanabe, Shirin Kalimuddin, Jenny G. Low, Subhash G. Vasudevan, Ann-Marie Chacko

> “...Infected mice were injected i.v. with 10 MBq [18 F]FDG and tissues were harvested following a 60-min tracer uptake. Freshly isolated wholemount lymphoid tissues were immediately exposed to multi-purpose phosphoscreen (BAS-IP MS) for 30 min. Fresh tissues with high tracer uptake were exposed to super-resolution (BAS-IP SR) phosphoscreen for 5 min (GE Healthcare Life Sciences, USA). [8 F]FDG standards at 2/3 serial dilution from 600 to 0 kBq were mounted together with mouse tissue for calibration of digital autoradiography (DAR) images. Screens were then scanned using the Sapphire Biomolecular Imager (Azure Biosystems, USA) at 100-µm resolution...”

Eur J Nucl Med Mol Imaging. 2022;49(13):4516-4528

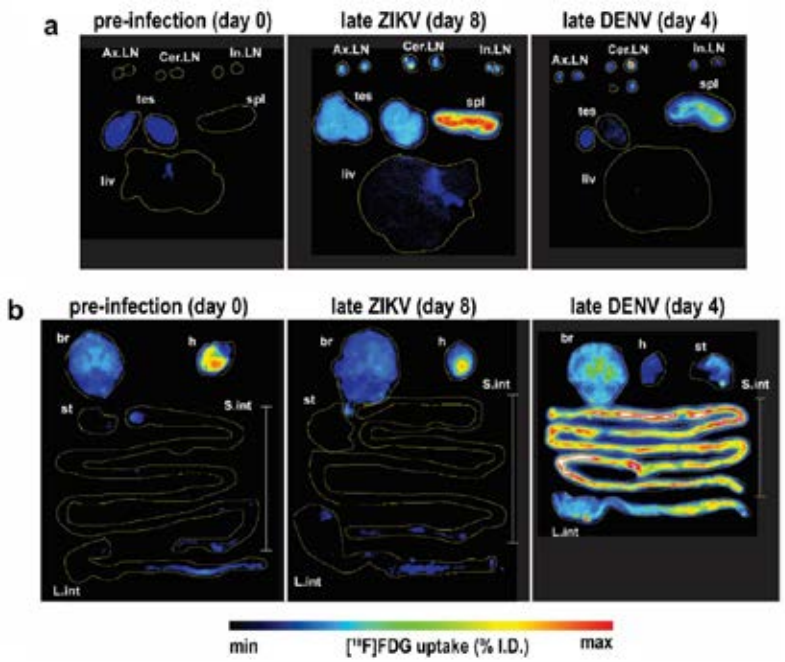

Figure 3. Ex vivo assessments of tissue [18F]FDG uptake in acute ZIKV and DENV disease. a, b Representative wholemount tissue ex vivo digital autora-diography (DAR) images of a lymphoid tissues, testes, and liver and b brain, heart, and digestive tract from pre-infection (n = 5), late ZIKV (n = 6), and late DENV (n = 8) mice.

Abbreviations: DENV, dengue virus; ZIKV, Zika virus.

THIN LAYER CHROMATOGRAPHY

PLOS ONE

Identification and functional analysis of a galactosyltransferase capable of cholesterol glycolipid formation in the Lyme disease spirochete Borrelia burgdorferi

Petronella R. Hove, Forgivemore Magunda, Maria Angela de Mello Marques, M. Nurul Islam, Marisa R. Harton, Mary Jackson, John T. Belisle

> "...The lipid extracts were resolved by thin-layer chromatography (TLC) using silica gel G60 TLC plates and chloroform/methanol (90:10 v/v) as the mobile phase. Reference non-radioactive standards were resolved concurrently and developed separately from the blot containing radioactive lipids with phosphomolybdic acid stain. Following this, blot with reference standard was matched with TLC blot to mark resolution of lipids. After development radiolabeled lipids were imaged using Azure Sapphire Biomolecular Imager (Azure Biosystems Inc, Dublin, CA)..."

PLoS One. 2021;16(6):e0252214

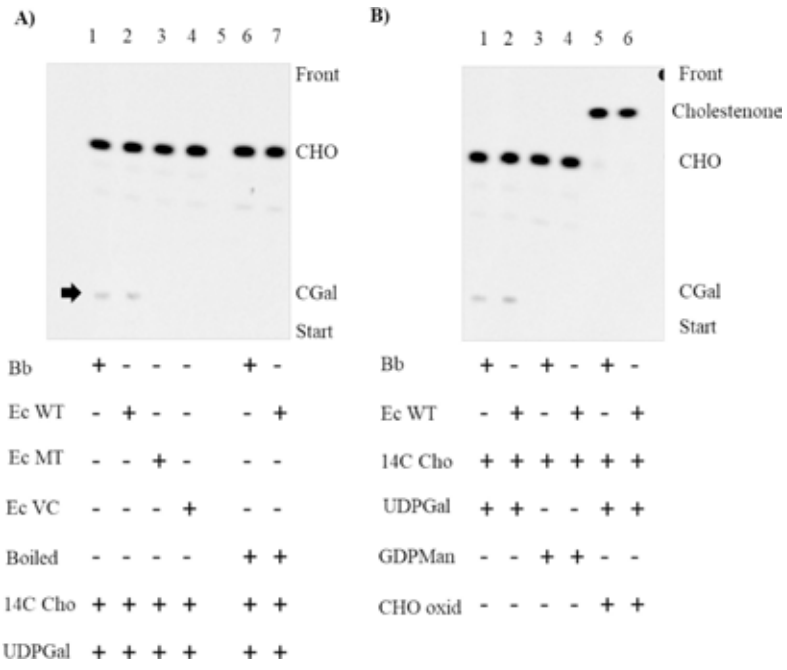

Figure 5. TLC of lipids from cell free assays for the enzymatic incorporation of [26- 14C] cholesterol into cholesteryl-β-D-galacto-pyranoside (CGal). A. The formation of cholesteryl-β-D-galactopyranoside (CGal) (arrow) in whole cell lysates of Bb and recombinant E. coli expressing WT bb0572 (lane 1 and 2). As expected, CGal was not formed by the whole cell lysate of E. coli expressing mutant bb0572 ΔCFF/I/DGD (lane 3). Lane 4 is the empty expression vector control, and lane 6 and 7 are from boiled whole cell lysates of Bb and recombinant E. coli expressing WT bb0572, respectively. Note lane 5 was not used. B. Substrate controls: Bb and E. coli WT bb0572 whole cell lysates with UDP-Gal (lane 1 and 2); GDP-Man (lanes 3 and 4), or cholesterol oxidase treated [26- 14C] cholesterol with UDP-Gal (lane 5 and 6) as substrate. CHO, cholesterol; ACGal, cholesteryl 6-O-acyl-β-D-galactopyranoside and MGal, monogalactosyl diacylglycerol. Ec WT (Escherichia coli wild type), Ec MT (E.coli mutant—bb0572 ΔCFF/DGD/I) and Ec VC- E.coli vector control).

LATERAL FLOW IMMUNOASSAY DEVELOPMENT

A novel rapid detection for SARS-CoV-2 spike 1 antigens using human angiotensin converting enzyme 2 (ACE2)

Jong-Hwan Lee, Minsuk Choi, Yujin Jung, Sung Kyun Lee, Chang-Seop Lee, Jung Kim, Jongwoo Kim, Nam Hoon Kim, Bum-Tae Kim, Hong Gi Kim

"...the intensity of the test and control lines were converted to peak histograms using a Sapphire Biomolecular Imager."

Biosens Bioelectron. 2021;171:112715

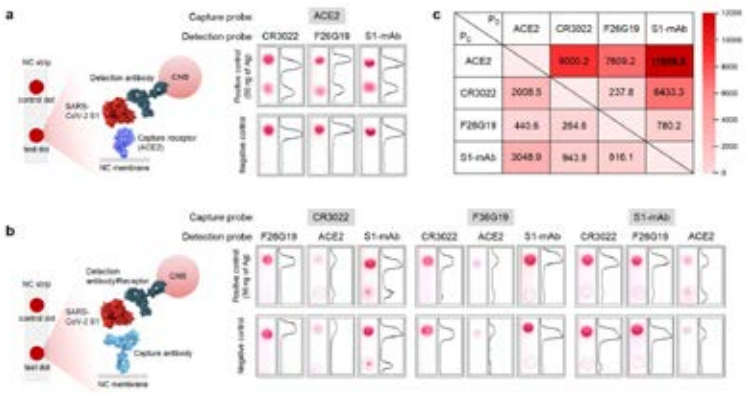

Figure 4. Identification of the sandwich pair for detection of SARS-CoV-2 spike antigen. a) Schematic diagram of LFIA using ACE2 as the capture probe and sandwich analysis results obtained from paired antibodies (CR3022, F26G19, and S1mAb). SARS-CoV-2 S1 antigen (50 ng) was used as a positive control, and buffer containing no S1 antigen was used as a negative control. After 20 min, the strips were captured by a smartphone, and their peak intensities were analyzed. b) Schematic diagram of LFIA, using antibodies as the capture probe, and their sandwich analysis results. c) Peak intensities of capture probe (PC)–detection probe (PD) pairs. A total of 12 pairs of positive controls (50 ng S1 antigen) were tested, and their intensities were analyzed. Peak intensity was calculated by subtracting the background intensity of the strip from the average intensities of the dots.

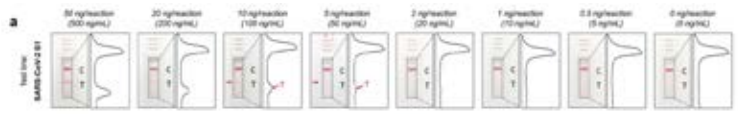

Figure 5a. Sensitivity and specificity of the ACE2-based LFA. a) Results of ACE2-based LFA for the detection sensitivity of SARS-CoV-2 S1 antigen. Serially diluted antigen concentrates (concentration range: 500 ng/mL to 5 ng/mL) were tested by ACE2-based LFA. After 20 min, the LFA strips were photographed with a smartphone. Moreover, the intensity of the test and control lines was converted to a peak histogram by an image analyzer.

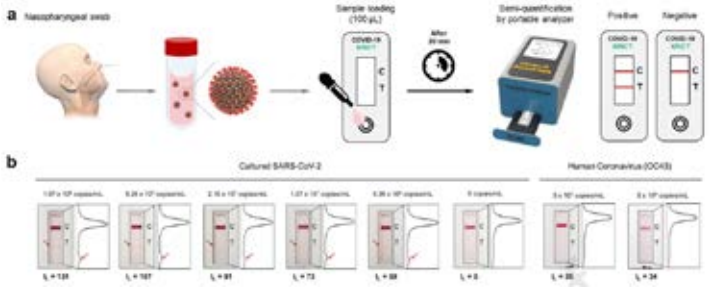

Figure 6b. Laboratory confirmation of ACE2-based LFIA using clinical samples. b) Results of ACE2-based LFA for the detection sensitivity of cultured SARS-CoV-2. Serially diluted virus concentrates (concentration range: 1.07×10^8 copies/mL to 5.35×10^6 copies/mL) were tested. After 20 min, the LFIA strip was taken with a smartphone and scanned with an image analyzer. The line intensities of the test and control lines were converted to peak histograms. Also, the intensity of the test lines was measured by a portable line analyzer (IL: line intensity of test line). Furthermore, human coronavirus (OC43) was tested as a negative control.

CLONOGENIC ASSAY

cancers

A novel rapid detection for SARS-CoV-2 spike 1 antigens using human angiotensin converting enzyme 2 (ACE2)

Jong-Hwan Lee, Minsuk Choi, Yujin Jung, Sung Kyun Lee, Chang-Seop Lee, Jung Kim, Jongwoo Kim, Nam Hoon Kim, Bum-Tae Kim, Hong Gi Kim

"...The clonogenic recovery potential gives insight into the capability of the cells to form a new tumor (metastasis). Therefore, 500 cells/well were seeded on a 6-well-plate and treated for 10 days with ART. Untreated cells served as controls. RCC cells were subsequently fixed with 85% MeOH/15% AcOH and stained with Coomassie (0.5 g Coomassie Blue G250 (Sigma-Aldrich, Darmstadt, Germany), 75 mL AcOH, 200 mL MeOH, 725 mL distilled water). Amount and size of cell clone colonies were measured with a biomolecular imager (Sapphire, Azure Biosystems, Biozym, Hess. Oldendorf, Germany)..."

Cancers. 2020;12(11):3150

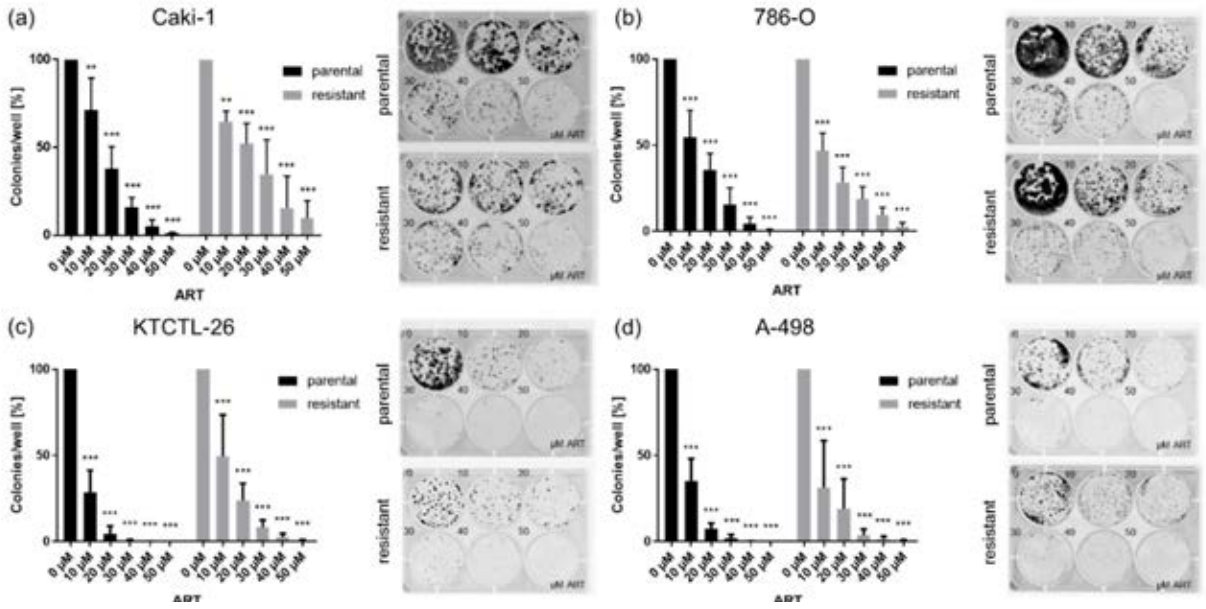

Figure 3. Clonogenic growth of RCC cells: Clonogenic growth of parental and resistant Caki-1 (a), 786-O (b), KTCTL-26 (c), and A 498 (d) cells treated with ART (10–50 µM) for 10 days. Untreated cells served as controls (set to 100%). Error bars indicate standard deviation (SD). Significant difference to untreated control: ** $p \leq 0.01$, *** $p \leq 0.001$. n = 5.

TABLE OF DYES

Visible Fluorescence

CellROX Deep Red	Neutrophils incite and macrophages avert electrical storm after myocardial infarction	*Nat Cardiovasc Res.*
Cell Tracker Green	Assessment of PI3K/mTOR/AKT Pathway Elements to Serve as Biomarkers and Therapeutic Targets in Penile Cancer	*Cancers*
Alexa Fluor® 488	ZnO Nanowire-Based Early Detection of SARS-CoV-2 Antibody Responses in Asymptomatic Patients with COVID-19	*Advanced Materials Interfaces*
Alexa Fluor® 546	Comparative Study of Bacterial SPOR Domains Identifies Functionally Important Differences in Glycan Binding Affinity	*Journal of Bacteriology*
Alexa Fluor® 647	Parallel imaging of coagulation pathway proteases activated protein C, thrombin, and factor Xa in human plasma	*Chem. Sci.*
Bodipy™ FL	SARS-CoV-2 M^{pro} inhibitors and activity-based probes for patient-sample imaging	*Nature Chemical Biology*
Bodipy™ PC	Phospholipase Dα1 Acts as a Negative Regulator of High Mg^{2+}-Induced Leaf Senescence in Arabidopsis	*Front Plant Sci.*
Cy5	Plasma proteomics reveals an improved cardio-metabolic profile in patients with type 2 diabetes post-liraglutide treatment	*Sage Journals*
	The mouse mammary tumor virus intasome exhibits distinct dynamics on target DNA	*bioRxiv*
	Parallel imaging of coagulation pathway proteases activated protein C, thrombin, and factor Xa in human plasma	*Chemical Science*
Cy3	Plasma proteomics reveals an improved cardio-metabolic profile in patients with type 2 diabetes post-liraglutide treatment	*Sage Journals*
	Parallel imaging of coagulation pathway proteases activated protein C, thrombin, and factor Xa in human plasma	*Chemical Science*
Cy2	Plasma proteomics reveals an improved cardio-metabolic profile in patients with type 2 diabetes post-liraglutide treatment	*Sage Journals*
FAM	A noncanonical RNA-binding domain of the fragile X protein, FMRP, elicits translational repression independent of mRNA G-quadruplexes	*Journal of Biological Chemistry*
	Method for the elucidation of LAMP products captured on lateral flow strips in a point of care test for HPV 16	*Analytical and Bioanalytical Chemistry*
Flamingo	Defensin-driven viral evolution	*Plos Pathogens*
Fluorescein	Early Drug Discovery and Development of Novel Cancer Therapeutics Targeting DNA Polymerase Eta (POLH)	*Front. Oncol.*
GelRed®	A slow-exchange conformational switch regulates off-target cleavage by high-fidelity Cas9	*bioRxiv.org*
GFP	Membrance stretching activates calcium permeability of a putative channel Pkd2 during fission yeast cytokinesis	*Molecular Biology of the Cell*
mCherry	Analyzing (Re)Capping of mRNA Using Transcript Specific 5 End Sequencing	*Bio-protocol*
SYBR™ Green	Method for the elucidation of LAMP products captured on lateral flow strips in a point of care test for HPV 16	*Analytical and Bioanalytical Chemistry*
SYBR™ Gold		
TMRE	Neutrophils incite and macrophages avert electrical storm after myocardial infarction	Nat Cardiovasc Res.

NIR Fluorescence

Azure Spectra 700	Alboserpin, the Main Salivary Anticoagulant from the Disease Vector Aedes albopictus, Displays Anti–FXa-PAR Signaling In Vitro and In Vivo	*ImmunoHorizons*
Azure Spectra 800		
Cy5.5	A phage mechanism for selective nicking of dUMP-containing DNA	*PNAS*
Cy7	A broadly neutralizing antibody protects Syrian hamsters against SARS-CoV-2 Omicron challenge	*Chemical Science*
DyLight™ 650	A broadly neutralizing antibody protects Syrian hamsters against SARS-CoV-2 Omicron challenge	*Nature Communications*
IRDye 680	*https://www.vetmed.ucdavis.edu/sites/g/files/dgvnsk491/files/inline-files/Weiss%20-%20STAR%20Poster.pdf*	
IRdye 800		

SAPPHIRE PUBLICATIONS OVERVIEW

492 PUBLICATIONS

As of July 14, 2023

300 Western blot	14 Northern blot	13 Southern blot
5 In-cell Western	42 Phosphor imaging	3 Total protein normalization

azure biosystems

6747 Sierra Court, Suites A-B • Dublin, CA 94568 USA
Phone: 925.307.7127 • Fax: 925.905.1816
info@azurebiosystems.com • www.azurebiosystems.com

MM-0139 R1